Sustainable Hydraulics in the Era of Global Change – Erpicum et al. (Eds.)
© 2016 Taylor & Francis Group, London, ISBN 978-1-138-02977-4

Estimation of 1D-confluence model parameters in right-angled discordant beds' confluences using 3D numerical model

D. Đorđević
Faculty of Civil Engineering, University of Belgrade, Belgrade, Serbia

I. Stojnić
(CERIS) – Instituto Superior Técnico – TU Lisbon, Portugal
LCH – EPFL, Lausanne, Switzerland

ABSTRACT: Parameters of 1D confluence models are originally defined for concordant beds' (CB's) confluences. This paper aims at estimating these parameters for discordant beds' confluences using numerical simulation results of 3D flow. A 3D finite-volume based model SSIIM2 that was successfully validated in CB's confluences is applied in this study, too. Confluences with the low, moderate and maximal observed bed elevation discordance ratio values are analysed for three characteristic hydrological scenarios: dominance of the tributary flow, equal contributions of the combining flows and dominance of the main-river flow. It is shown that: 1) the mean flow angle $\bar{\delta}$ approaches junction angle α with the increase in bed elevation discordance, especially when tributary flow dominates, 2) the value of Hager's correction coefficient σ is not constant and 3) the contribution of the tributary flow to the 1D momentum equation is under predicted when either parameter $\bar{\delta}$ or σ is used for its estimation.

1 INTRODUCTION

Extensive bathymetric surveys in river confluences during mid-1980s revealed that there was a difference in bed elevations between the tributary and main channels in the majority of surveyed confluences (Kennedy, 1984). The difference was created through a combined effect of the deposition of coarse sediment particles that had been arriving from upstream channel and deepening of the scour hole at the entrance to the post-confluence channel due to enhanced turbulence caused by collision of the combining flows (Con-stantinescu et al., 2011). The presence of the bed step at the tributary entrance to the confluence affects momentum transfer from the tributary to the main-river. A proper estimation of this influence is of crucial importance for an accurate prediction (calculation) of upstream water levels (flow depths) in 1D flow modelling of dendritic river networks and lengthy river reaches. However, existing 1D-confluence models that were intended for the treatment of a confluence as an internal boundary condition in such analyses had been developed for the concordant beds' case, i.e. for the case when bed elevations of the combining channels are equal. The early models of Taylor (1944), Weber and Greated (1965) and Lin and Song (1979) did not take into account the fact that the tributary flow deflected from the junction angle as it entered the main-river. Those proposed after 1980 (Hager, 1987, 1989; Ramamurthy et al., 1988; Gurram et al., 1997; Hsu et al., 1998a, b and Gurram & Karki, 2000) encountered the tributary flow deflection in calculating its contribution to the momentum equation for the direction of the main-river flow either by introducing the correction coefficient σ for the junction angle α (Hager, 1987, 1989 and Gurram et al., 1997), or by observing pressure difference between the opposite tributary walls near the confluence (Ramamurthy et al., 1988) or, by introducing mean cross-sectional value of the flow deflection angle in the downstream section of the tributary channel (Hsu et al., 1998a, b). All these models resulted from the combination of theoretical analysis and experiments. Experiments were used to estimate and recommend values of key parameters and/or variables that were necessary for the proper inclusion of the momentum transfer from the tributary to the main-channel. However, to draw general conclusions about model parameters extensive laboratory experiments or field measurements are needed. Since the preparation and performance of laboratory experiments might be costly, Đorđević (2014) considered a possibility of using a 3D numerical model as a substitute to a physical model in studying the confluence hydrodynamics and in estimating parameters of 1D-confluence models. The study undoubtedly confirmed that a 3D finite-volume based model SSIIM2 was a reliable predictive tool in concordant beds' confluences. Moreover it confirmed once again the dependence of Hager's parameter σ on the discharge ratio $D_R = Q_{MR}/Q_d$ (where Q_{MR} is the discharge in the main-river upstream

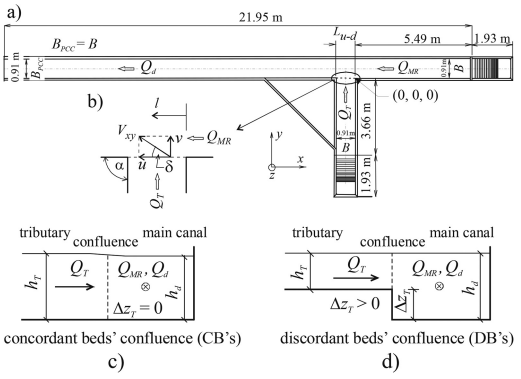

Figure 1. a) Planform of Shumate's (1998) laboratory confluence, b) definition sketch for the flow angle δ, c) concordant bed's confluence, d) discordant beds' confluence.

of the confluence, and Q_d is the total downstream discharge) in the 90° confluence – a feature that had not been fully discussed and underlined in original papers of Best and Reid (1987) and Hager (1989).

This paper continues the line of Đorđević's previous study (2014), by analysing the effect of bed elevation discordance on the values of parameters from 1D concordant beds' confluence models of Hager, Gurram et al. and Hsu et al. One can conclude from Best and Reid's and Hager's studies that there is a dual dependence of the junction angle correction coefficient σ on the junction angle α, and the discharge ratio D_R. However, it is intuitively obvious that the elevated channel bed of the tributary with the backward facing step at its downstream end results in increased momentum of the tributary flow and thus in its ability to keep its original direction. This paper will show how the extent of the bed elevation discordance affects the average flow deflection angle of the tributary flow on the horizontal plane ($\bar{\delta}$) and its correction coefficient σ. Additionally, the paper will attempt to evaluate the discrepancy between values of the component of the tributary force of inertia that acts in the main river direction (I_{Tx}) obtained from different 1D models and that calculated by integration of the corresponding component of the momentum flux over the downstream tributary cross-section.

To keep up with the previous study, a layout from Shumate's 90° concordant beds' confluence of equal width laboratory canals with rectangular cross-section and horizontal beds is also used in this analysis (Fig. 1a). In addition to the original confluence layout ($\Delta z_T/h_d = 0.00$), three different hypothetical layouts with the following values of the bed elevation discordance ratio $\Delta z_T/h_d = \{0.10, 0.25, 0.50\}$ are analysed (where Δz_T stands for the difference in bed elevations between the tributary and main canals and h_d for the flow depth in the main canal in the confluence, Figs 1c, d). Values of the average δ-angle ($\bar{\delta}$) and the component I_{Tx} of the force of inertia in the downstream tributary cross-section are deduced from the numerical simulation results for the three different D_R values: $D_R = \{0.250, 0.583, 0.750\}$. Results are obtained with the 3D finite-volume based model SSIM2 that was previously successfully validated against the data from laboratory (Biron et al., 1996) and field (Đorđević, 2010) discordant beds' confluences.

Since 1D-confluence models of Hager (1987), Gurram et al. (1997) and Hsu et al. (1998a) were recalled and briefly presented in the previous study they will not be repeated here. Thus, the paper proceeds with the description of the setup of numerical experiments (section 2) and the presentation of the numerical modelling details (section 3). Values of the characteristic parameters and variables for confluences with different extent of bed elevation discordance are compared in section 4. Additionally, equations for the best fitting curves for Hagers's σ "coefficient" are given. Finally the most important conclusions drawn from this study are summarised.

2 SETUP OF NUMERICAL EXPERIMENTS

A right-angled laboratory confluence of two straight canals with horizontal concordant beds (Shumate, 1998) is used as a starting point in this study (Figs 1a, c). Such a choice follows from the successful validation of the SSIIM2 model with the experimental data from this facility. Hypothetical, discordant beds' confluences are formed by elevating the bed of the lateral canal for the amount of Δz_T (Fig. 1d). The bed step height Δz_T is chosen such that the bed elevation discordance ratio $\Delta z_T/h_d$ does not exceed the maximal observed value in river confluences, i.e. the value of 0.50 (Biron and Lane, 2008). In addition to this value, two values that correspond to moderate ($\Delta z_T/h_d = 0.25$) and low ($\Delta z_T/h_d = 0.10$) extents of bed elevation discordance are selected for this study. To allow comparison with parameters for the concordant beds' case, numerical simulations are performed with the input data from experiments with $D_R = Q_{MR}/Q_d = \{0.250, 0.583, 0.750\}$. The total, downstream discharge and the flow depth at the downstream end of the main canal were the same in all experiments ($Q_d = 0.17\,\mathrm{m^3/s}$, $h_{out} = 0.296\,\mathrm{m}$).

3 NUMERICAL MODELLING

Flow in discordant beds' confluences is simulated using 3D finite-volume based model SSIIM2 (Olsen, 2012). This model solves a set of equations which consists of the mass conservation equation, Reynolds-averaged Naiver-Stokes equations and turbulence model equations that are used to close the system of conservation laws. The standard $k-\varepsilon$ model is used as a turbulence model closure in this paper. Equations are solved on an unstructured multiblock space grid. The SSIIM 2 model uses SIMPLE method to couple the mass and momentum equations. Since there is no other option available, the rigid-lid approach is used to represent the free-surface. Such a treatment

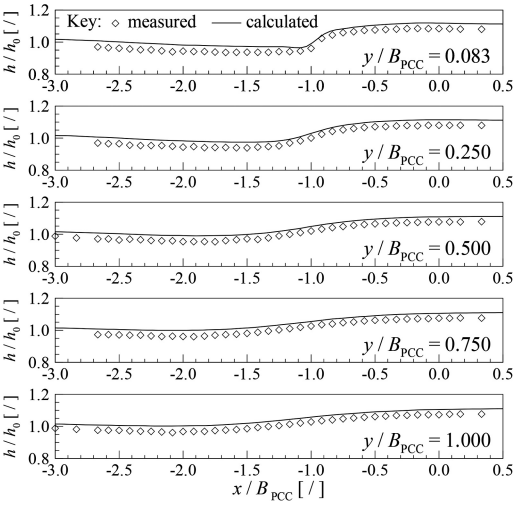

Figure 2. Comparison of the measured and calculated non-dimensional water surface profiles at different non-dimensional lateral distances (y/B_{PCC}) from the junction-side wall in Shumate's experiment with $D_R = 0.583$.

of the free-surface is justified by a good agreement between numerical simulation results and measurements as shown in Đorđević & Biron (2008), Đorđević (2013, 2014). Validation against Shumate's experiments has shown that values of simulated velocities are within confidence interval which corresponds to the significance level of 0.05 (Đorđević 2014). Such a good agreement is additionally confirmed in this paper by comparison of the simulated and measured non-dimensional free-surface profiles for $D_R = 0.583$ (Fig. 2). It is readily noticeable that the agreement between each of the two profiles is acceptable for the concordant beds' case. Discrepancies are below 4%. Similar results are obtained for the other two D_R-values. Thus, it is reasonable to believe that the free-surface treatment by the rigid-lid approach would also result in a good estimation of pressures at the rigid-lid in discordant beds' cases i.e. good prediction of both velocity fields and the free-surface. Convective terms in the momentum equations are modelled in the same manner as in the previous study, i.e. with the second-order upwind scheme.

Boundary conditions are prescribed as follows. A constant discharge is set at each inflow boundary and a constant depth is set at the outflow boundary. Remaining dependent variables at the outflow boundary are determined from the zero gradient condition. This condition is also applied for ε and horizontal velocities at the free-surface, while the zero discharge condition is used to calculate the vertical velocity component. The turbulence kinetic energy at the free-surface is set to the half of its bottom value (Olsen, 2000). The treatment of solid boundaries rests on the wall-law.

The computational domain in all simulations covers full lengths of the two canals (Fig. 1a). As it was the case in laboratory experiments, such a choice ensured no influence of boundary conditions on the flow within the confluence hydrodynamic zone (i.e. zone within and downstream of the confluence where effects of the collision between and combining of the two flows are felt). The multiblock space grid has two blocks each of which is an orthogonal structured grid. The block 1 covers the main canal, whereas block 2 covers lateral, tributary canal. The size of block 1 is, therefore, the same for all confluence layouts – it has 838 cells in the stream-wise, 37 cells in the lateral and 20 cells in the vertical directions. The vertical size of block 2 reduces with an increase in the bed elevation discordance ratio, while the horizontal size remains unaltered – 183 cells in the stream-wise and 37 cells in the lateral directions. Table 1, summarises the grid size in block 2 for the four considered confluence layouts. The presented block dimensions were accepted after grid sensitivity analysis based on the value of the GCI (Đorđević, 2013).

Table 1. Grid size in block 2 for the four analysed confluence layouts.

Case No.	$\Delta z_T/h_d$ [/]	Grid size in block 2	Type of confluence
1	0.00	183×37×20	Concordant beds'
2	0.10	183×37×18	
3	0.25	183×37×15	Discordant beds'
4	0.50	183×37×10	

4 RESULTS AND DISCUSSION

Parameters of 1D-confluence models (i.e. the mean cross sectional flow deflection angle $\bar{\delta}$ in the model of Hsu et al. and the correction coefficient σ in models of Hager and Gurram et al.) and the component of the tributary force of inertia that acts in the direction of the mean-channel flow (I_{Tx}) are estimated from the calculated velocities u and v in the downstream tributary cross-section (Fig. 1b).

Mean cross-sectional angle $\bar{\delta}$ and correction coefficient σ. The mean flow angle on the horizontal plane $\bar{\delta}$ is calculated by averaging the δ-angle over the cross-section. To do this a cross-sectional distribution of the δ-angle should be known. The distribution is found by calculating the value of this angle in each point of computational mesh in the downstream tributary cross-section from the basic trigonometric relation: $\delta = \text{arc tg}(v/u)$. Rather than presenting these distributions for the twelve cases, variations of mean values for 38 cross-sectional verticals are given in Figure 3. It is readily noticeable that the greatest variations within the cross-section are present when the main-river flow dominates ($D_R = 0.750$, Fig. 3c) and that the least flow deflection might be expected when there is a dominance of the tributary flow ($D_R = 0.250$, Fig. 3a). For the given D_R-value, the variation reduces with the increase in the extent of

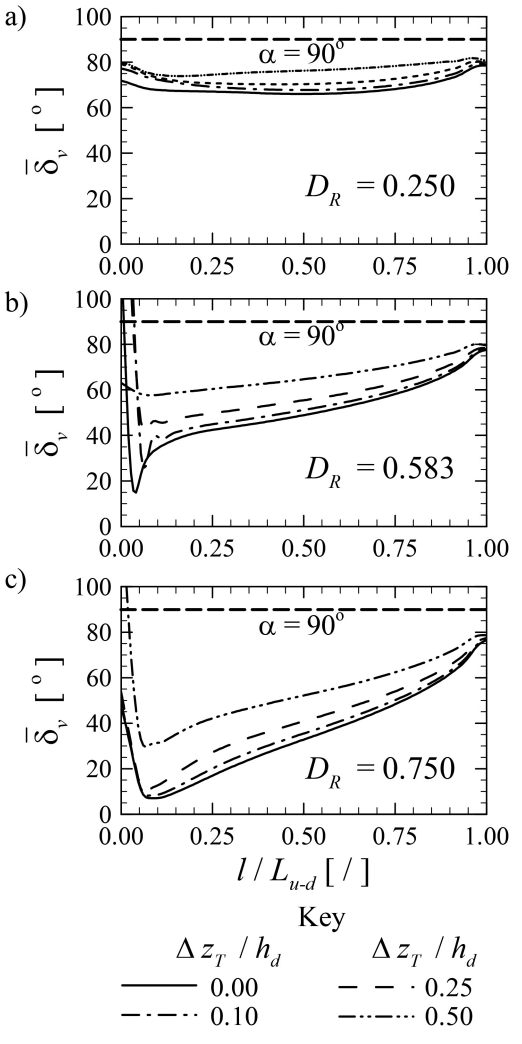

Figure 3. Effect of bed elevation discordance ratio $\Delta z_T/h_d$ on the variation of mean δ-angle values in verticals of the downstream tributary cross-section for different hydrological scenarios (D_R-values).

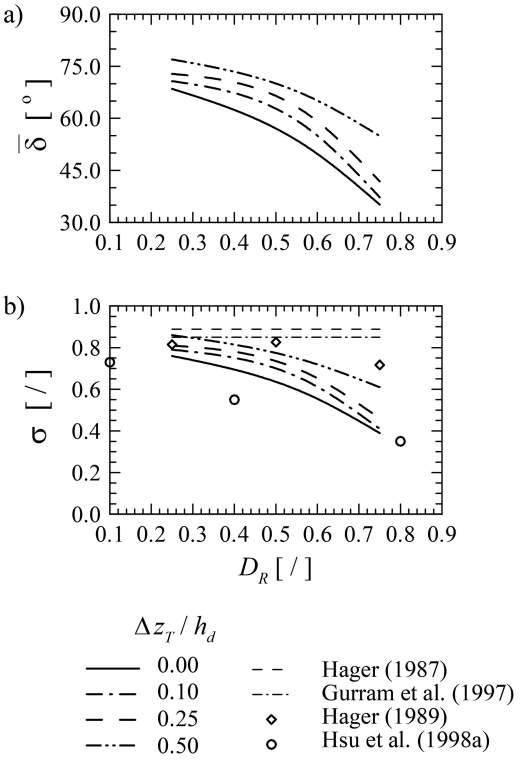

Figure 4. Effect of bed elevation discordance ratio $\Delta z_T/h_d$ on a) mean cross-sectional flow angle $\bar{\delta}$ and b) correction coefficient σ for different hydrological scenarios (D_R-values).

bed elevation discordance ($\Delta z_T/h_d$). For example, the greatest deflection from the junction angle α happens in the vertical located at $l = 0.08L_{u-d}$ in the concordant beds' case ($\Delta z_T/h_d = 0.00$) when $D_R = 0.750$. The mean flow angle in this vertical ($\bar{\delta}_v$) is only 7°, i.e. the flow deflects from the junction angle by $\alpha - \bar{\delta}_v = 83°$. For low and moderate extents of bed elevation discordance (i.e. for $\Delta z_T \leq 0.25h_d$) there is no significant difference in comparison with the concordant beds' case ($\min \bar{\delta}_v \approx \{8°, 11°\}$ for $\Delta z_T = \{0.10, 0.25\}$). The minimal flow angle $\bar{\delta}_v$ in this vertical increases approximately four times when $\Delta z_T/h_d$ reaches its maximal value of 0.50 ($\min \bar{\delta}_v = 30°$). Consequently, the mean cross-sectional flow angle $\bar{\delta}$ is increased by almost 60% (from ≈33° for $\Delta z_T = 0.00$ to ≈53° for $\Delta z_T = 0.50h_d$, Fig. 4a). Cross-sectional variations are still notable for the hydrological scenario with almost equal contributions of the two combining flows ($D_R = 0.583$) as long as $\Delta z_T \leq 0.25h_d$ (Fig. 3b). For $\Delta z_T = 0.50h_d$ variations across the canal width become negligible as in the case when tributary flow dominates ($D_R = 0.250$, Fig. 3a). However, the average flow deflection from the junction angle is still greater (24°) than that in the concordant beds' confluence (21°) when $D_R = 0.250$. Reduced $\bar{\delta}_v$-angle variations result in greater cross-sectional mean values: $\bar{\delta} \in$ [≈50°, ≈65°] for $\Delta z_T \in [0.00, 0.50]h_d$ (Fig. 4a). When compared to the case with $D_R = 0.750$, a percentage increase in the $\bar{\delta}$-angle value between $\Delta z_T = 0.00$ and $\Delta z_T = 0.50h_d$ is halved. With further increase in dominance of the tributary flow ($D_R = 0.250$), the average deflection from the junction angle becomes almost constant along more than $0.50L_{u-d}$. The least flow deflection (of only 13°) happens again when $\Delta z_T = 0.50h_d$. A percentage increase in the mean cross-sectional δ-angle value between the concordant beds' confluence and the confluence with $\Delta z_T = 0.50h_d$ is halved again when compared to the case with $D_R = 0.583$, and the range of $\bar{\delta}$-angle values is reduced: $\bar{\delta} \in$ [≈66°, ≈76°] for $\Delta z_T \in [0.00, 0.50]$ h_d. (Fig. 4a).

The correction coefficient σ changes with D_R and $\Delta z_T/h_d$ in the same manner as $\bar{\delta}$ (Fig. 4b). Such a behaviour follows from its definition: $\sigma = \bar{\delta}/\alpha$. It is

Table 2. Coefficients of the best fitting curves for the σ-coefficient ($\sigma = aD_R^3 + bD_R^2 + cD_R + d$).

	$D_R \in [0.250, 0.583]$				$D_R \in [0.583, 0.750]$			
$\Delta z_T/h_d$	a	b	c	d	a	b	c	d
0.00	−1.52	1.14	−0.68	0.88	3.04	−6.83	3.96	−0.019
0.10	−2.51	1.88	−0.67	0.88	5.01	−11.28	7.00	−0.611
0.25	−2.51	1.88	−0.61	0.88	5.01	−11.28	7.06	−0.606
0.50	−0.99	0.74	−0.47	0.95	1.96	−4.42	2.54	0.361

interesting to notice that the value of the σ-coefficient is generally less than proposed constant values of Hager (8/9) and Gurram et al. (0.85), except in the confluence with $\Delta z_T = 0.50 h_d$ when $D_R = 0.250$. In this case, σ approaches Gurram et al.'s value of 0.85, and exceeds corresponding value from Hagers's amended curve by 6%. Additionally, σ-value in the discordant beds' confluence with $\Delta z_T = 0.25 h_d$ approaches the value from Hagers's amended curve when $D_R = 0.250$. For $D_R > 0.40$ σ-curves are always between Hager's amended and Hsu et al.'s curves. It seems that both Hager and Gurram et al. overestimated $\bar{\delta}$-angle values, because they deduced them from the point measurements with a miniature angle meter at the mid-depth where variability of the δ-angle is less pronounced than that in the bottom layers. As for comparison with Hsu et al.'s data it is should be mentioned that the tributary canal was narrower than the main-canal, in their experiments which, most probably, resulted in greater variability of the $\bar{\delta}$-angle and, thus, lower σ-coefficient values. Table 2 summarises information on best fitting curves for the four analysed confluence layouts. The best fitting curves are cubic polynomials: $\sigma = aD_R^3 + bD_R^2 + cD_R + d$. Curves are defined in the two ranges of D_R-values: $D_R \in [0.250, 0.583]$ and $D_R \in [0.583, 0.750]$.

Tributary force of inertia and its components. Components of the tributary force of inertia are calculated through the integration of corresponding momentum fluxes over the downstream tributary cross-section and the magnitude of the total force of inertia is then found from: $I_T = (I_{Tx}^2 + I_{Ty}^2 + I_{Tz}^2)^{1/2}$. In this particular case, the cross-section is a vertical plane with the normal in the y-direction (Fig. 1a). Thus, the momentum of the tributary flow is carried to the main-canal by the velocity component in the y-direction, i.e. by the v-velocity. This further means that the momentum flux through the elemental surface $\mathrm{d}A_y$ is described for each coordinate direction only with one term from every momentum conservation equation. The flux in the direction of the main-canal axis is described by the term $\rho uv\mathrm{d}A_y$ from the momentum equation in x-direction, that for the lateral direction is described by the term $\rho vv\mathrm{d}A_y$ from the equation for the y-direction, while the term $\rho wv\mathrm{d}A_y$ from the equation for the z-direction describes the flux through $\mathrm{d}A_y$ in the vertical, z-direction. The latter two components are relevant only for the calculation of the total force of inertia (I_T), while the one in the x-direction is of interest for the 1D confluence flow modelling.

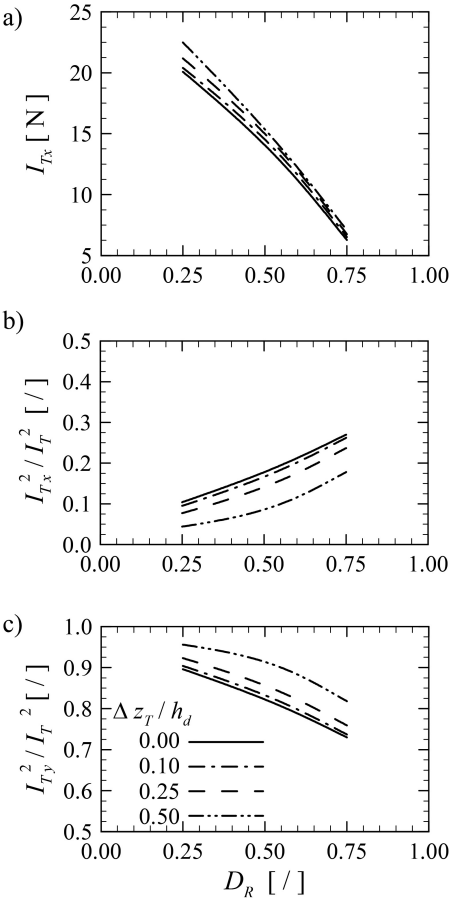

Figure 5. a) Variation of the I_{Tx} magnitude with D_R and $\Delta z_T/h_d$, b) contribution of the I_{Tx} magnitude to the magnitude of the total force of inertia I_T, c) contribution of the I_{Ty} magnitude to the magnitude of the total force of inertia I_T.

A variation of the I_{Tx} magnitude with D_R and $\Delta z_T/h_d$ is presented in Figure 5a. One can observe from this figure that the I_{Tx} magnitude decreases with the increase in dominance of the main-river flow regardless the bed step height at the tributary entrance to the confluence and that it increases with the increasing extent of the bed elevation discordance between the two canals for the given D_R-value. However, such an observation may be misleading in deriving conclusions about the effect of $\Delta z_T/h_d$ on the contribution

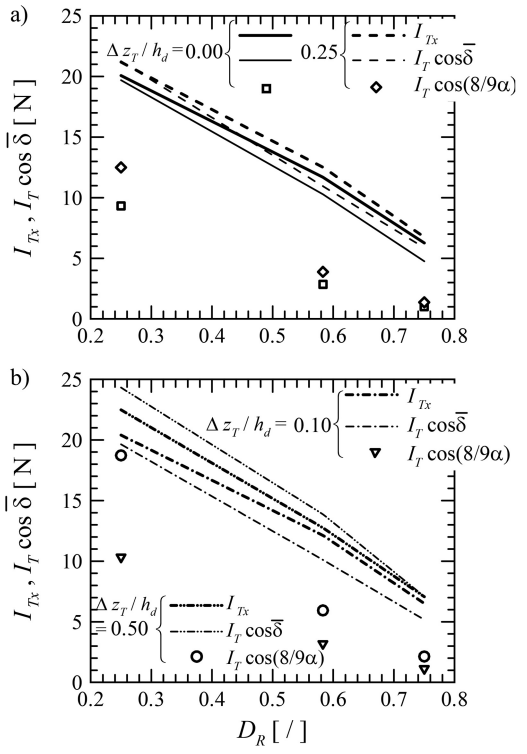

Figure 6. Comparison of the force of inertia I_{Tx} to its estimates based on the mean cross-sectional flow angle $\bar{\delta}$ (Hsu et al.) and the proposed σ correction coefficient value of 8/9 (Hager).

of the tributary force of inertia to the 1D momentum equation. Therefore, a contribution of the I_{Tx} magnitude to the magnitude of the total force of inertia I_T is presented in Figure 5b. This figure shows what was intuitively expected. Firstly, that the increased deflection of the tributary flow, when the main-canal flow dominates ($D_R = 0.750$, Figs 2c and 3a), results in greater contribution of the I_{Tx} component to the total force of inertia, and, thus, greater contribution of the tributary flow to the 1D momentum equation. Secondly, the momentum in the direction of the tributary canal, i.e. in the y-direction, increases with the increasing extent of the bed elevation discordance (Fig. 5c). This results in much smaller contribution of the I_{Tx} component to the I_T. The amount of reduction increases with the increasing dominance of the tributary flow, i.e. decrease in D_R (Table 3).

The force of inertia I_{Tx} is compared to its estimates based on the mean cross-sectional flow angle $\bar{\delta}$ (Hsu et al.) and the proposed σ correction coefficient value of 8/9 (Hager) in Figure 6. It is readily noticeable that the I_{Tx} value is under predicted no matter which parameter is used for its estimation as long as $\Delta z_T \leq 0.25 h_d$. The use of the $\bar{\delta}$-angle results in either over prediction ($\Delta z_T = 0.50 h_d$) or under prediction ($\Delta z_T \leq 0.25 h_d$) of I_{Tx}. The over prediction does not exceed 10% and the under prediction does not exceed 25%. However,

Table 3. The effect of D_R and $\Delta z_T/h_d$ on the percentage reduction of the I_{Tx} contribution to I_T when compared to the concordant beds' case.

	D_R [/]		
$\Delta z_T/h_d$ [/]	0.250	0.583	0.750
0.10	8.5	5.3	3.3
0.25	26.3	17.9	12.3
0.50	58.2	46.8	34.3

when the constant σ-value is used, the value of I_{Tx} component is under predicted with more than 40%. The percentage reduction in some cases may reach 84%. Therefore, the use of the constant σ value is not recommended except in confluences with the greatest bed elevation discordance ratio when the tributary flow dominates ($\Delta z_T = 0.50 h_d$ and $D_R = 0.250$). In such a case the percentage reduction is of the same order as that obtained with $\bar{\delta}$. Such a behaviour is a direct consequence of the already observed tendency of the σ-curve to approach proposed constant σ-value of Gurram et al. in the confluence with $\Delta z_T = 0.50 h_d$ at low D_R values (Fig. 4b).

5 CONCLUSIONS

A 3D finite-volume based numerical model SSIIM2, which had been successfully applied in the previous study for estimation of 1D confluence model parameters in right-angled concordant beds' confluence, was used in this paper for estimation of these parameters in discordant beds' confluences with the same planform geometry. The comparison with the results for the concordant beds' confluence led to the following conclusions:

1. The increase in bed elevation discordance ratio $\Delta z_T / h_d$ reduces variation in the flow angle δ in the downstream tributary cross-section. Consequently, the mean cross-sectional flow angle $\bar{\delta}$ is increased.
2. The amount of this increase, when compared to the concordant beds' case, depends on the D_R-value. The greatest effect is achieved for $D_R = 0.750$, i.e. when the main-river flow dominates. The $\bar{\delta}$-angle in increased by 60% at maximum (i.e. from $\bar{\delta} = 33°$ for $\Delta z_T = 0.00$ to $\bar{\delta} \approx 53°$, for $\Delta z_T = 0.50 h_d$). The maximum increase is successively halved for the remaining two D_R-values. For $D_R = 0.583$, the $\bar{\delta}$-angle value of $\approx 50°$, when $\Delta z_T = 0.00$, is increased to $\approx 65°$, when $\Delta z_T = 0.50 h_d$. This range is significantly narrowed when $D_R = 0.250$, i.e. $\bar{\delta} \in [66°, 76°]$ for $\Delta z_T \in [0.00, 0.50] h_d$.
3. Values of the correction coefficient σ are generally less than constant values of 8/9 and 0.85 proposed by Hager and Gurram et al., respectively. Moreover, they lay between the amended curve of Hager and that derived from experiments of Hsu et al. The only exception is the confluence with the

greatest observed bed elevation discordance ratio ($\Delta z_T = 0.50 h_d$) when the tributary flow dominates ($D_R = 0.250$). In this case the σ-value approaches the value 0.85 as proposed by Gurram et al.

4. The contribution of the tributary flow to the 1D momentum equation that is written for the main-river direction reduces in the discordant beds' confluences with the increase in bed elevation discordance ratio, because of the reduced variation of the flow angle $\bar{\delta}$ in the downstream tributary cross-section.
5. The use of the mean cross-sectional flow angle $\bar{\delta}$ and the correction coefficient σ for the estimation of the component of the tributary force of inertia that acts in the direction of the main-canal flow may lead to significant under prediction of the contribution of the tributary flow to the 1D momentum equation. The under prediction of the I_{Tx}-value may be as high as 84% when the constant σ-value of Hager is used. Therefore, it is recommended to use neither of proposed constant σ-values. Rather a variable σ-value, deduced from the $\bar{\delta}$-angle value, might be used, as the discrepancy between I_{Tx} and $I_T \cos\bar{\delta}$ would not exceed 25%.

REFERENCES

Best, J.L., and Reid, I. 1987. Closure to Separation zone at open channel junctions, *J. Hydraul. Eng*., ASCE, 113, 4, 545–548.

Biron, P.M. & Lane, S.N. 2008. Modelling hydraulics and sediment transport at river confluences. In: Rice, S.P., Roy, A.G. & Rhoads, B.L. (Eds.) *River confluences, tributaries and the fluvial network*. Wiley, 17–38.

Constantinescu, G., Miyawaki, S., Rhoads, B., Sukhodolov, A. and Kirkil, G. 2011. Structure of turbulent flow at a river confluence with momentum and velocity ratios close to 1: Insight provided by an eddy-resolving numerical simulation, *Water Resour. Res.* 47, 9W05507, doi:10.1029/2010WR010018.

Đorđević, D. 2010. *Numerical investigation of the river confluence hydrodynamics*. Unpublished PhD Dissertation, University of Belgrade, Belgrade, 382p

Đorđević, D. 2013. Numerical study of 3D flow at right-angled confluences with and without upstream planform curvature. *J. of Hydroinformatics*, 15.4: 1073–1088.

Đorđević, D. 2014. Can a 3D-numerical model be used as a substitute to a physical model in estimating parameters of 1D confluence models?, *Proc. 3rd IAHR Europe Congress*, Porto, 158–167.

Gurram, S.K., Karki, K.S., and Hager, W.H. 1997. Subcritical junction flow, *J. Hydraul. Eng*., ASCE, 123, 5, 447–455.

Gurram, S. K. and Karki, S. K. 2000. Discussion of Subcritical open-channel junction flow, *J. Hydraul. Eng.,* ASCE, 126, 1, 87–89.

Hager, W.H. 1987. Discussion of Separation zone at open-channel junctions, *J. Hydraul. Eng*., ASCE, 113, 4, 539–543.

Hager, W.H. 1989. Transitional flow in channel junctions, *J. Hydraul. Eng*., ASCE, 115, 2, 243–259.

Hsu, C.C., Wu, F.S. and Lee, W.J. 1998a. Flow at 90^o equal-width open-channel junction, *J. Hydraul. Eng.,* ASCE, 124, 2, 186–191.

Hsu, C.C., Lee, W.J. and Chang, C.H. 1998b. Subcritical open-channel junction flow, *J. Hydraul. Eng*., ASCE, 124, 8, 847–855.

Lin, J.D. and Soong, H.K. 1979. Junction losses in open channel flows, *Water Resour. Res.*, 15, 2, 414–419.

Kennedy, B. 1984. On Playfair's law of accordant junctions. *Earth Surface Processes and Lanforms*, 9: 153–173.

Olsen, N.R. 2000. *CFD Algorithms for Hydraulic Engineering*. Trondheim: The Norwegian University of Science and Technology.

Olsen, N.R. 2012. *A three-dimensional numerical model for simulation of sediment movements in water intakes with multi-block option – User's Manual*, The Norwegian University of Science and Technology, Trondheim.

Ramamurthy, A.S., Carballada, L.B. and Tran, D.M. 1988. Combining open channel flow at right angled junctions, *J. Hydraul. Eng.*, ASCE, 114, 12, 1449–1460.

Shumate, E.D., 1998. *Experimental description of flow at an open-channel junction*. Unpublished Master thesis, Univ. of Iowa, Iowa, 150 p.

Taylor, E.H. 1944. Flow characteristics at rectangular open-channel junctions, Transactions, ASCE, 109, 893–912.

Weber, N.B. and Greated, C.A. 1965. An investigation of flow behaviour at the junction of rectangular channels, *Proc. Instn. of Civ. Eng.*, Thomas Telford Ltd, London, 34, 321–334.